18èmes Journées Internationales de Thermique (JITH 2017)
Monastir (Tunisie), 25 - 27 Octobre 2017

Evaluation of the performance of a membrane distillation system coupled with solar energy

Evaluation des performances d'un système de distillation membranaire couplé à l'énergie solaire

Nader FRIKHA, Samira BEN ABDALLAH, Slimane GABSI
Unit of research: Environment, Catalysis and Processes Analysis, National Engineering School of Gabes, Gabes University, Street Omar Ibn ElKhattab - 6029 Gabes, Tunisia
naderfrikha@yahoo.fr, *abdallahsamira@yahoo.com*, *slimane.gabsi53@gmail.com*

Abstract : In this work we propose to estimate the potential of vacuum membrane distillation of seawater coupled with solar energy. We compare the performance of a desalination system coupling a flat sheet module to three different solar technologies: plat solar collector, cylindro-parabolic collector and solar pond. A model describing the operation with the three solar technologies has been proposed. The model was established on the basis of assessments of mass transfer and heat transient. From this model we developed a simulation program that evaluates and compare the performance of the different configurations. This study also quantified the production of the system with and without recycling the retentate.

Keywords : solar energy, desalination, membrane plane, vacuum membrane distillation, modeling.

1. Introduction

Desalination using solar energy coupled with membrane technology is considered an attractive alternative for the production of drinking water especially in rural and arid areas. Membrane distillation (MD) is a thermal membrane separation process which uses hydrophobic porous membranes to separate a solution physically. The process driving force is the difference between the vapor pressure between the two sides of the membrane [1, 2]. The hydrophobic nature of the membrane prevents liquid solutions from entering its pores due to the surface tension forces. As a result, liquid/vapor interfaces are formed at the entrances of the membrane pores. The principle of separation by MD is based on the liquid/vapor equilibrium which controls the selectivity of the process [3-6].

The principal interests of MD compared to other popular separation processes are the lower operating temperatures than the conventional distillation, the lower operating pressures than the pressure-driven processes, the less demanding membrane mechanical properties and the high rejection factor achieved when solutions containing no-volatile solutes [7,8], as well as the greater contact specific area due to the installation compact nesses, the modularity and the possibility of automating the process easily.

The crisis of drinking water announced for the coming years raise the interest of rapid development of desalination technologies cheaper, simpler, more robust, more reliable and less energy intensive and environmentally friendly. In this context, we studied three configurations of desalination units using DMV technology and coupling a flat membrane module (flat sheet module) with different solar technologies.

2. Configurations studied

For vacuum membrane distillation technology, the required temperature is usually below 80 °C, this temperature can be provided by most solar thermal collectors. We studied three types of solar collectors: flat solar collector, cylindro-parabolic collector and solar pond.

Figure 1 shows the schematic principle of the studied configurations. The role of a thermal solar collector is to transform the solar radiation received into useable heat energy, usually via a coolant. The restitution of a part of the collected energy is performed by passing of a coolant in one or more tubes in contact with a metallic absorber. The coolant allows the heating the sea water in a heat exchanger.

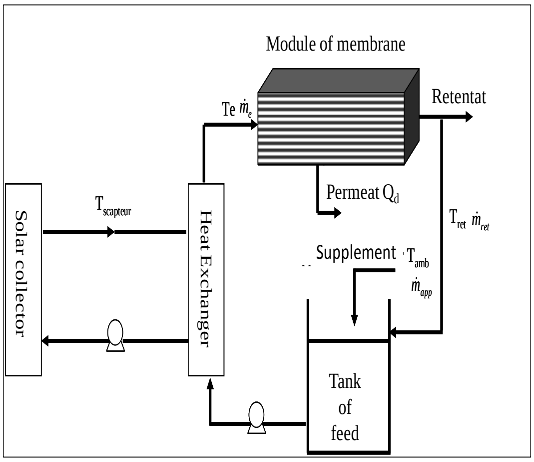

Figure 1: Diagram of the desalination unit

A tank used to mix the supplement seawater and retentate. This mixture is heated at the heat exchanger, and then it feeds the membrane module. The vapor produced is condensed in a condenser placed downstream of the membrane module. The retentate can be discarded or recycled, and two operating modes are possible: Operation with or without recycling.

3. Dynamic modeling of solar technologies

3.1. Flat solar collector

To develop a model describing the temperature distribution for a flat solar collector in transient state, energy balances on the absorber and on the coolant are established. These balances lead to a system of two equations that reflect the evolution of the fluid temperature T_{Fd} and of the absorber T_{Ab} along the collector as a function of time [9]:

$$\begin{cases} \dfrac{\partial T_{Ab}(z,t)}{\partial t} = \dfrac{1}{\rho_{Ab} S_{Ab}\ Cp_{Ab}}\left[h_{Fd}\pi d_{in}(T_{Fd}-T_{Ab}) + Ul_{Ab}(f(t)-T_{Ab})\right] \\ \dfrac{\partial T_{Fd}(z,t)}{\partial t} = v_{Fd}\dfrac{\partial T_{Fd}(z,t)}{\partial z} + \dfrac{h_{Fd}}{\rho_{Fd}\ Cp_{Fd}\ \dfrac{d_{in}}{4}}(T_{Ab}-T_{Fd}) \end{cases} \tag{1}$$

Where f (t) represents the function:

$$f(t) = \frac{\alpha\tau G_i(t)}{U} + T_{amb} \tag{2}$$

and S_{Ab} the area of heat accumulation :

$$S_{Ab} = \frac{\pi}{4}\left(d_{ex}^2 - d_{in}^2\right) + l_{Ab}e \tag{3}$$

With

C_p: Heat capacity

U : Overall heat transfer coefficient

h_{Fd} : Heat transfer coefficient

v_{Fd} : Velocity

d_{int} , d_{ext} : Internal and external diameters

l_{Ab} , e : Width and thickness of the absorber plate

T_{amb} : Ambient temperature

The solar radiation G_i was calculated on the basis of the EUFRAT model and validated by the climatic data of the Sfax region [10].

3.2. Cylindro-parabolic collector (CPC)

The absorber is the main component in the CPC, which has the function of absorbing the incident solar radiation, to convert it into heat and transmit it to a heat transfer fluid.

A heat transfer equation between the absorber and the water leads to a partials differentials equations [11]:

$$\begin{cases} \dfrac{\partial T_{Ab}(t)}{\partial t} = \dfrac{G_i(t)\, w_{CPCc}}{\rho_{Ab} Cp_{Ab} \dfrac{\pi}{4}\left(d_{ex}^2 - d_{in}^2\right)} - \dfrac{4 h_e\, d_e}{\rho_{Ab} Cp_{Ab}\left(d_{ex}^2 - d_{in}^2\right)}\left(T_{Ab} - T_{amb}\right) - \dfrac{4 h_i\, d_i}{\rho_{Ab} Cp_{Ab}\left(d_{ex}^2 - d_{in}^2\right)}\left(T_{Ab} - T_F\right) \\ \dfrac{\partial T_F(z,t)}{\partial t} = -v_F \dfrac{\partial T_F(z,t)}{\partial t} + \dfrac{h_i}{\rho_{Fd}\, Cp_F\, d_{in}}\left(T_{Ab} - T_F\right) \end{cases} \quad (4)$$

With
h_e , h_i the heat transfer coefficients
T_{ab}: absorber temperature
T_F: fluid temperature
T_{amb}: ambiant temperature
w_{CPC} : diameter of CPC
v: fluid velocity

3.3. Solar pond

Solar pond is a large solar collector with integrated heat storage. In practice, a solar pond is a salt water pool which has three distinct zones (Figure 2). The first zone, located at the top of the pond, contains the low density saltwater mixture. This zone is called the upper convective zone (UCZ) which is the absorption and transmission region. The second zone which contains a variation of salinity increasing with depth is the gradient zone or non-convective zone (NCZ). This zone acts as an insulator to prevent heat from escaping to the UCZ, maintaining higher temperatures at lower zones.

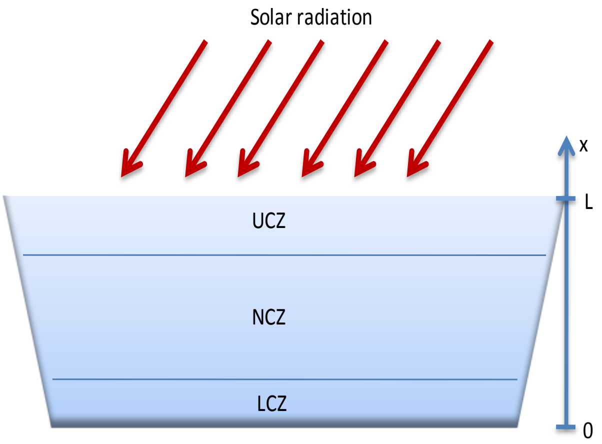

Figure 2 : Schematic diagram of a solar pond

The balances of mass and heat on the pond leads to the following system of partial differential equations [12]:

$$\begin{cases} \dfrac{\partial(\rho_{sw} Cp_{sw} T_{sw}(t,x))}{\partial t} = \lambda_{sw} \dfrac{\partial^2 T_{sw}(t,x)}{\Delta^2 x} + 0{,}6 \mu_{ex} G_i\, e^{-\mu_{ex}(L-x)} \\ \dfrac{\partial(\rho_{sw} S)}{\partial t} = D \dfrac{\partial^2 (\rho_{sw} S)}{\partial^2 x} \end{cases} \quad (5)$$

with
ρ_{SW}: salt water density
μ_{ex}: extension coefficient
Cp_{sw} : salt water heat capacity
Tsw: salt water temperature
S: salinity
λ: heat conductivity
D: coefficient of salt diffusion

4. Dynamic modeling of flat sheet module

The membrane module is a device assembling a number of compartments separated by hydrophobic porous sheet membranes. The membranes are mounted on either side of rigid frames, stacked according to the principle of the filter press. This arrangement provides a lot of flexibility, and good access to the membranes for cleaning or replacement. Each membrane is located between a water compartment in which circulates the water to be desalinated and an under reduced pressure compartment connected to a vacuum creating system (vacuum pump, liquid ring pump ...). This second compartment is used for recovering water vapor (Figure 3).

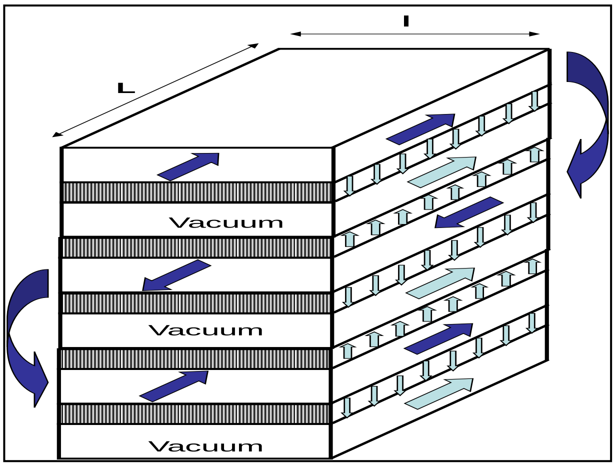

Figure 3: Schematic diagram of flat sheet module

Thus a module having n membranes comprise (n+1)/2 compartments, half of the compartments will be devoted to the fluid and the other half is reserved for recovery of the permeate. We will take an odd number of membranes in order to have the same number of compartments for the feed water and for the vacuum.

4.1. Assumptions

For the calculation of energy balance, the following assumptions were taken into account: The saturated vapor pressure P_{ws} can be expressed using the equation of Antoine [13]. P_{ws} is in Pa and the temperature Tz is in Kelvin.

$$P_{ws} = \exp\left(A_1 - \frac{A_2}{T - A_3}\right) \qquad (6)$$

with A_1= 23,1964 A_2= 3816,44 A_3 = 46,13

The transfer of water molecules in the gas phase through the pores of the membrane is by the Knudsen diffusion mechanism [14, 15].

At the sea water-membrane interface, there will be evaporation at the temperature (T_m). The vapor generated passes through the vacuum compartment and we assume that the vapor temperature dominates the vacuum compartment. Thus, we have the temperature in the vacuum-membrane interface (T_{vacuum}) equal to the temperature of sea water-membrane interface (T_m).

$$T_m = T_{vacuum} \qquad (7)$$

- The coefficient of permeability of the membrane k_m (Knudsen permeability) is a function of temperature at the interface of the membrane (T_m) and can be expressed as follows [16, 17, 18]:

$$k_m = \frac{2}{3}\frac{\varepsilon r}{\chi\delta}\sqrt{\frac{8}{R\pi}}\frac{1}{\sqrt{T_m}} \qquad (8)$$

With ε the membrane porosity, δ the thickness, χ the tortuosity and r pore radius.

k_{m0} is the permeability coefficient calculated at a reference temperature T_0.

$$k_m = k_{m0}\sqrt{\frac{T_0}{T_m}} = K\,T_m^{-0,5} \quad \text{with} \quad K = k_{m0}\,T_0^{0,5} \qquad (9)$$

All physico-chemical properties of the fluid change depending on the temperature and salinity.

4.2. Permeate flux density

The flux density of water vapor through the internal interface membrane-water (kg.s^{-1}.m^{-2}) is described by the following equation:

$$J_v = k_m \Delta P = k_m \left[P_i - P_{vacuum}\right] \quad (10)$$

Where P_i is the partial pressure of water at the membrane interface. The partial pressure is written as a function of the activity coefficient and the mass fraction of the water or salt.

$$P_i = \alpha_{water/NaCl} X_{water} P_{ws} = \gamma_{water/NaCl} \left(1 - X_{NaCl}\right) P_{ws} \quad (11)$$

The activity coefficient of water $\gamma_{water/NaCl}$ depends on the salinity of the solution to be treated [19].

$$\gamma_{water/NaCl} = 1 - 0{,}5 X_{NaCl} - 10 X_{NaCl}^2 \quad (12)$$

The salt mass fraction can be expressed as a function of the salinity and the molar masses of water and salt by the following expression:

$$X_{NaCl} = \frac{1}{1 + \frac{M_{water}}{M_{NaCl}} \left(\frac{\rho_{solution}}{C_{NaCl}} - 1 \right)} \quad (13)$$

So we can write the expression for the permeate flux density as follows:

$$J_v = K T_m^{-0,5} \left[\gamma_{water/NaCl} \left(1 - X_{NaCl}\right) \exp\left(A_1 - \frac{A_2}{T_m - A_3} \right) - P_{vacuum} \right] \quad (14)$$

4.3. Mass balance

The transfer of matter inside the module is caused by pressure difference across the membrane. The evolution of the distillate flow along the modules can be written as follows:

$$\frac{d\dot{m}_{dist}}{dz} = Pe\, J_v \quad (15)$$

Pe: membrane perimeter wetted by the feed solution

Wetted perimeter for a planar membrane module is given by:

$$Pe = n_{membrane}\, l \quad (16)$$

4.4. Heat balance

The heat balance in transient state applied to an elementary volume dV of the module is written as follows:

$$\dot{m}_{feed,z} Cp_l \left(T_z - T_{ref}\right) = \dot{m}_{feed,z+dz} Cp_l \left(T_{z+dz} - T_{ref}\right) + \left(\dot{m}_{feed,z} - \dot{m}_{feed,z+dz}\right) L_v + \rho_l dV Cp_l \frac{d\left(T_z - T_{ref}\right)}{dt} \quad (17)$$

By combining the two balance equations (Eq 15, Eq 17), we obtain the final equation that describes the evolution of the retentate temperature over time and space:

$$\frac{dT_z}{dt} = -v_z \frac{dT_z}{dz} - \frac{4 J_v}{\rho_l\, Cp_l} \frac{S}{V} \left[Cp_l \left(T_{ref} - T_z\right) + L_v \right] \quad (18)$$

S and V respectively designate the membrane surface and volume available to the liquid.

v_z is the velocity of seawater to the z position:

$$v_z = \frac{\dot{m}_{feed,z}}{\rho_l\, S_{passage}} \quad (19)$$

We assume that the surfaces of module in contact with the ambient environment are well insulated so that we can neglect transfers outward. $\left(\frac{dT}{dr} = 0, \frac{dT}{dx} = 0 \right)$

The volume available to the fluid in any module is a function of the passage section:

$$V = L\ S_{passage} \tag{20}$$

The membrane surfaces available and the passage sections are given by the following expressions:

$$S = LPe = n_{membrane} l\, L \tag{21}$$

$$S_{passage} = n_{membrane}\ e\ l \tag{22}$$

The resolution of the two differential equations based on the coupling of the heat and mass balances will allow the determination of the produced amount of distillate and the liquid temperature along the membrane module.

$$\dot{m}_{dist} = \int J_v\ Pe\ dz \tag{23}$$

5. Results

There are several ways to solve a system of partial differential equations nonlinear. In our case the regressive method of finite differences was used. The method consists in discredited the equations in order to have a matrix that contains the terms of the system. This matrix is solved by the iterative method of Gauss Seidel. Three simulation programs were developed on the calculation software MATLAB.

We propose to study two operating modes: with and without recycling.

5.1. Operation without recycling

The membrane module comprises 3 planar membranes each with an area of 0.5 m^2. The compartments have a thickness of 5 cm. It is assumed that the walls of the membrane module are well insulated and heat losses to the outside are also neglected.

Figure 4 shows the daily production for the 4 typical days in the case of a module powered by a CPC collector array with a total collecting area of 70 m^2. We note that the distillate flow varies according to the season. For the month of June, maximum distillate flow is 18 kg·h^{-1}.m^{-2} while for the month of December it is 8.3 kg·h^{-1}.m^{-2}. This is mainly due to the variation of the output of the solar collector temperature, which depends on the received solar radiation and the efficiency of the solar collector.

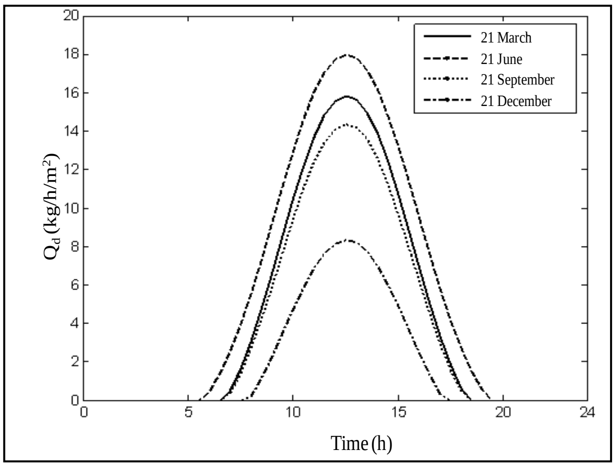

Figure 4: Variation of the distillate flow density Variation of the distillate flow density without recycling

S_{cap} = 70 m^2,S_{mem} = 1.5 m^2

The comparison of annual productivity obtained by the three solar collectors show the best configuration is that of the CPC, followed by solar pond and finally the collector flat (table 1). This is justified, taking into account temperature levels obtained at the output of the 3 types solar collectors.

Table 1: Annual production for operation without recycling

	Flat collector	*CPC*	*Solar pond*
Annual production (m^3.m^{-2})	13.3	31,8	13,6

Taking into account the collecting area, productivity per unit of membrane surface and per unit of collector surface is relatively low. This is explained by the complete rejection of retentate which has a relatively high temperature. The collecting area may be reduced in the case of operation with recycling.

5.2. Operation with recycling

We propose to study the operation of flat sheet module with total recycling of the retentate. The adopted installation comprises a flat membrane module, a flat plate collector having a collecting area of 2 m^2, a heat exchanger and a tank of 500 L. The module used has a length of 0.383 m, a width of 0.21 m and a thickness of 0.033m. It consists of 27 membranes and 14 water compartments. We have worked with a flow rate of 808 kg / hr at the inlet of the first compartment; this flow ensures a velocity inside the module of 1 m / s. The retentate exiting a compartment feeds the next compartment. Figure 5 shows the temporary evolution of the distillate flow density for the typical days: March 21, June 21, September 21 and December 21. From Figure 5, we see that the maximum distillate flow during the day varies according to the season. Note that for the month of September the maximum distillate flow rate was 25 kg/h/m^2 while for December it is 17 kg/h/m^2. Simulations of operation with recycling have shown that we can improve production. Indeed, if we take the example of June 21 we observe that the maximum permeate flux density has increased from 18 kg/h/m^2 without recycling about 24 kg/h/m^2 with recycling.

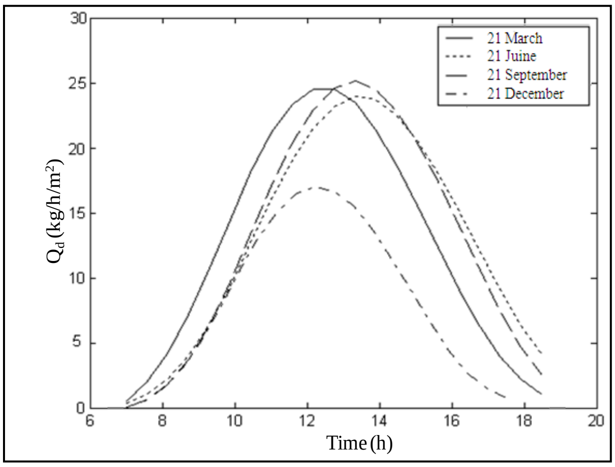

Figure 5: Variation of the distillate flow density with recycling

S_{cap} = 2 m^2,S_{mem} = 2.17 m^2

This improvement is explained by the recovery of sensible heat of the retentate leaving the membrane module at a high temperature. We note that the operating with total recycling will not be appropriate in practice due to the excessive accumulation of salt in the tank. This accumulation will result in clogging of membrane. Thus the choice of an optimum recycling rate allowing both to improve production without harming the membrane will be of great interest.

On the other hand, the average productivities of the days of March 21, 21 June and 21 September are very close. We note that production improvement is noticed mainly in the first five compartments; indeed heat transfer between compartments is very limited because the vacuum compartment limits any heat transfer by conduction.

Conclusion

To develop a model describing the functioning of the flat sheet module coupled with solar energy, we developed three models for different types of solar collectors: flat solar collector, cylindro-parabolic collector and solar pond. A model describing the operation of membrane module was also developed. The different models are based on balance equations of mass and heat under transient conditions. From these models, we developed calculation programs on the software MATLAB and this in order to simulate and study the functioning of three configurations of membrane vacuum distillation. The models developed are able to determine the evolution of temperatures and the flow rate of distillate during time and for any day of the year the day. The comparison of performance of the different configurations studied showed that the CPC is the most efficient solar collector. Indeed with 70 m^2 of collecting area we estimate an annual production of about 31.8 m^3 per m^2 of membrane. Furthermore, the study showed that recycling of the retentate increases the production of a remarkably. Indeed recycling allows recovering sensible heat of the retentate leaving the membrane module at a relatively high temperature. The prospects consist essentially in determining the performance of flat sheet module integrated in the absorber of the solar collector or submerged at the solar pond.

References

[1] R.B. Saffarini, E.K. Summers, H.A. Arafat, J.H. Lienhard, 'Technical evaluation of stand-alone solar powered membrane distillation systems', Desalination, 286, pp 332–341, (2012).

[2] X. Yanga, R. Wanga, L. Shi, A.G. Fane, M. Debowski, 'Performance improvement of PVDF hollow fiber-based membrane distillation process', J. Membr. Sci., 369, pp 437–447, (2011).

[3] S. Al-Obaidani, E. Curcio, F. Macedonio, G. Di Profio, H. Al-Hinai, E. Drioli, 'Potential of membrane distillation in seawater desalination: thermal efficiency, sensitivity study and cost estimation', J. Membr. Sci., 323, pp 85–98, (2008).

[4] N. Couffin, C. Cabassud, V. Lahoussine-Turcaud, 'A new process to remove halogenated VOCs for drinking water production: vacuum membrane distillation', Desalination, 117, pp 233–245, (1998).

[5] M.S. El-Bourawi, Z. Ding, R. Ma, M. Khayet, 'A framework for better understanding membrane distillation separation process', J. Membr. Sci., 285, pp 4–29, (2006).

[6] K.W. Lawson, D.R. Lloyd, 'Membrane distillation', J. Membr. Sci., 124, pp 1–25, (1997).

[7] S. Adnan, M. Hoang, H. Wang, Z. Xie, 'Commercial PTFE membranes for membrane distillation application: Effect of microstructure and support material', Desalination, 284, pp 297–308, (2012).

[8] M. Khayet, 'Membranes and theoretical modeling of membrane distillation: A review', Adv. Colloid Interface Sci. 164, pp 56–88, (2011).

[9] N. Frikha., R. Matlaya, B. Chaouachi, S. Gabsi, Simulation of an autonomous solar vacuum membrane distillation for seawater desalination, Desalination and Water Treatment, 52, pp 1725-1734, (2013).

[10] S. Ben Abdallah, étude d'une unité de dessalement solaire membranaire sous vide: modélisation, simulation et optimisation des conditions opératoires. Theses ENIG, Tunisia, (2015)

[11] S. Ben Abdallah, N. Frikha, S. Gabsi, 'Study of the performances of different configurations of seawater desalination with a solar membrane distillation', Desalination and Water Treatment, pp 1-10, (2013).

[12] S. Ben Abdallah, N. Frikha, S. Gabsi, Numerical Investigations of Coupling a Vacuum Membrane Desalination System with a Salt Gradient Solar Pond, Journal of Fundamentals of Renewable Energy and Applications, 6, pp 1-8, (2016).

[13] B. Li, K.K. Sirkar, 'Novel membrane and device for vacuum membrane distillation-based desalination process', J. Membr. Sci., 257, pp 60–75, (2005).

[14] M.A. Abu-Zeid, Y. Zhang., H. Dong., L. Zhang., H.L. Chen., L. Hou., A comprehensive review of vacuum membrane distillation technique, Desalination, 356, pp 1-14, (2015).

[15] T.D. Dao, J.P. Mericq, S. Laborie, C. Cabassud., A new method for permeability measurement of hydrophobic membranes in Vacuum Membrane Distillation process, Water Research, 47, pp 2096-2104, (2013)

[16] D. Wirth, C. Cabassud, 'Water desalination using membrane distillation: Comparison between inside/out and outside/in permeation', Desalination, 147, pp. 139–145, (2002).

[17] L. Sun, L. Wang., Z. Wang., B. Li., S. Wang., Characteristics analysis of cross flow vacuum membrane distillation process, Journal of Membrane Science, 488, pp 30–39, (2015).

[18] M. Gryta, Effectiveness of water desalination by membrane distillation process. Membrane, 2, pp 415-429, (2012).

[19] K.W. Lawson, D.R. Lloyd, 'Membrane distillation', J. Membr. Sci., 124, pp 1–25, (1997).